Finite size effects in simulations of thermal conductivity under lower mantle conditions

Ben Todd,* Stephen Stackhouse, Andrew M. Walker, and Jon E. Mound

School of Earth and Environment, University of Leeds, United Kingdom

(Dated: November 15, 2017)

Abstract

Knowledge of thermal conductivity is important for modelling the deep earth, but can not be measured experimentally at core mantle boundary conditions. Atomic scale simulations sidestep experimental limitations, but system size must be chosen carefully in order to determine accurate conductivity values.

Here we investigate the effects of finite simulation size and show how conductivity can be over-estimated when using the direct method. EXTRAPOLATION PROCEDURE

WE FIND OTHER STUDIES MAY HAVE DONE STUFF WRONG BY NOT CONSIDERING FSE

Classical molecular dynamics approaches are utilised, with the intention of constraining system parameters for future ab-initio studies.

ADD RESULTS

TO DO:

SCALING LAW

GK AT 1000K

* Corresponding author: ee10bt@leeds.ac.uk

I. INTRODUCTION

A. Intro Intro (remove this subsection header later)

Knowledge of the thermal conductivity of solids is key in a wide range of technological applications and for our understanding of natural systems. For example, in the Earth's lower mantle thermal conductivity controls the nature of planetary convection (Tosi *et al.* [1]), and the heat flux out of the core which powers the geotherm. Low thermal conductivities are required in thermoelectric materials, to maximise the efficiency of heat-electricity conversion (Snyder and Toberer [2]).

A range of atomic scale simulation methods are available to determine the lattice thermal conductivity of materials. These are invaluable for calculating thermal conductivity at conditions of which experiments are difficult, e.g. the extreme conditions found in the Earth's lower mantle (pressures and temperatures up to 136 GPa and 4000 K at the core-mantle boundary).

(MOVE - to where though?) Many studies assume lowermost mantle thermal conductivity to be 10 $\mathrm{Wm^{-1}K^{-1}}$ (e.g. Lay *et al.* [3]), but uncertainty in the extrapolation of results made at low pressures and temperatures gives a range of 4 - 16 $\mathrm{Wm^{-1}K^{-1}}$ (Brown and McQueen [4], Osako and Ito [5], Hofmeister [6], Goncharov *et al.* [7], Manthilake *et al.* [8], Ohta *et al.* [9]).

B. Pre-intro to methods (remove this subsection header later)

Stackhouse and Stixrude [10] review different methods to compute thermal conductivity, in the present work we focus on two of these: (1) Equilibrium molecular dynamics based on the Green-Kubo relations to determine the thermal conductivity from heat flux fluctuations and their time-dependence (Green [11], Kubo [12, 13], Schelling *et al.* [14]REMOVE SCHELLING REFERENCE?). (2) The "direct method" based non-equilbrium molecular dynamics, where thermal conductivity is calculated from an imposed heat flux and corresponding temperature gradient via Fourier's Law (Muller-Plathe [15], Nieto-Draghi and Avalos [16]).

C. The question/motivation (remove this subsection header later)

Considering systems of varying size, length-dependent conductivities are obtained from the direct method and extrapolated to the bulk material (Schelling *et al.* [14]). The validity of this extrapolation procedure have been called into question (e.g. Sellan *et al.* [17]), when a linear trend cannot be fit through the length-dependent conductivities [THIS WHOLE PARAGRAPH IS WISHY-WASHY, SPECIFIC THINGS TO AS-YET-UNDISCUSSED DIRECT METHOD, NOT GENERAL STATEMENTS]. We describe finite-size effects (FSE) which cause the conductivity result of a simulation to diverge from the value expected by a linear trend, and offer a comparison with results obtained from the Green-Kubo method. The two methods have previously been compared (e.g. Schelling *et al.* [14] [[[REFERENCED EARLIER IN THIS PARAGRAPH, THIS OKAY?]]]), and have been found to give results in good agreement. [[[IMPORTANT FOR ABSTRACT]]]

D. Bridgmanite (remove this subsection header later)

(WHY ELSE IS BRIDG INTERESTING, OUTSIDE OF EARTH APPLICATIONS)(BRIDG ELECTRICAL/RADIATIVE CONDUCTIVITY)(HOW DOES BRIDG COMPARE TO MATERIALS IN OTHER FSE STUDIES) Bridgmanite, or $MgSiO_3$ (magnesium silicate) perovskite, comprises around 80% (75%? REF?) of the lower mantle (need to mention the other 20%?), and is an insulator past its Debye temperature at all conditions relevant to the deep earth (TRUE? REF?).

(((MOVE TO DISCUSSION?))) There have been several computational studies to calculate the lattice thermal conductivity of bridgmanite at CMB conditions. Our approach is similar to that of Ammann *et al.* [18], who use the direct method and interatomic potentials reporting a value of $\sim$8.5 $Wm^{-1}K^{-1}$. Stackhouse *et al.* [19] again use the direct method but with density functional theory, yielding conductivity of 6.8 ± 0.9 $Wm^{-1}K^{-1}$. Using Green-Kubo, Haigis [20] report a value of 12.4 ± 2.0 $Wm^{-1}K^{-1}$for conditions of 3000 K, 139 GPa. Tang *et al.* [21] and Dekura *et al.* [22] employed first principles, anharmonic lattice dynamics techniques, obtaining values of $\sim$1 $Wm^{-1}K^{-1}$(CMB conditions) and 2.3 $Wm^{-1}K^{-1}$(for 4000 K and 100 GPa) respectively. These results are much lower than other studies, and could be because of LD TRUNCATION OF CONDUCTIVITY [CRITICAL ANALYSIS].

E. Intro to rest of paper (remove this subsection header later)

In section II [[Section?]] we provide an overview of the methods and expand on issues. In section III we outline our computational approaches, for the non-equilibrium molecular dynamics direct method and equilibrium molecular dynamics Green-Kubo method. In section IV we show convergence of computed conductivity with respect to simulation cell size and shape (AND PRESSURE/TEMPERATURE EFFECTS?). ALSO IN RESULTS, DISCUSS SCALING LAW / THEORETICAL MODEL? In section V we suggest the minimum system parameters to be utilised in similar lower mantle studies, and discuss potential future work.

II. THEORY

A. Phonons (remove this subsection header later)

PHYSICS JOURNAL LEVEL? Heat is transported as lattice virbrations, or phonons. The further phonons travel before scattering (mean free path, MFP) the more efficient the heat transport, and thus the higher the thermal condutivity. A number of effects (MENTION MATTHIESSEN'S RULE) cause phonons to scatter: (1) collisions with other phonons in the lattice, (2) boundaries or defects in the material, and (3) impurities in the atomic structure. The finite-size effects we describe are associated with (1) [[[ALSO 2, BUT PERIODIC BOUNDARIES ARE DIFFERENT FROM GRAIN BOUNDARIES?]]], where simulation system sizes are too small to recreate the phonon-phonon scattering of the bulk material. The FSE observed for a material will change with thermal conductivity/phonon MFP, and thus are pressure, temperature, and composition sensitive (IS MENTIONING COMPOSITION RELEVANT?). Higher conductivity materials/conditions require larger systems to eliminate FSE (and vice versa) [[[BUT IS THIS TRUE? SHOULD IT BE IN THIS SECTION, OR DISCUSSION?]]]

B. Direct method (remove this subsection header later)

The direct method is the computational implementation of a typical experiment to measure thermal conductivity, using Fourier's law to relate heat flux (q) and temperature gra-

dient (∇T) to thermal conductivity (k),

$$q = -k\nabla T. \tag{1}$$

In the direct method energy is transferred from one group of atoms to another, creating hot and cold regions between which heat flows. The resultant temperature gradient is measured by calculating the temperature of individual groups of atoms along the direction of the heat flux. Simulation cells tend to be long relative to their cross-sectional area, defined as height by width. Cell boundaries are periodic and the hot and cold sections are half the cell length apart, meaning heat flows out of both ends of the cell from hot to cold. This results in two similar temperature gradients which can be averaged.

From kinetic theory ((REFERENCE??)), conductivities computed by the direct method (k_L) are dependent on length of simulation cell,

$$k_L = \frac{1}{3} C_V v l_L, \tag{2}$$

where C_v is the volumetric heat capacity, v is the average phonon drift velocity, and l_L is the phonon mean free path. The finite size of the simulation cell truncates the mean free path, underestimating conductivity compared to that of the bulk material (k_∞). Using results from simulations of varying cell length (L), conductivity is extrapolated to a length-independent value (where b is a material dependent parameter),

$$k_L{}^{-1} = bL^{-1} + k_\infty{}^{-1}. \tag{3}$$

Inverse conductivities from direct method simulations are plotted against corresponding inverse cell lengths. A straight line is fit to the data and extrapolated to the y-axis (at which the inverse cell length equals zero and real length equals infinity), where the intercept gives the inverse of the bulk material conductivity (Schelling *et al.* [14]).

Problems arise when the data does not support a linear trend. There are three effects of finite system size that cause an individual direct method simulation to diverge away from the inferred linear trend, both of which result in overestimation of the length-dependent conductivity. First, when the distance between hot and cold sections (controlled by cell length) is shorter than the MFP, phonons travel ballistically (i.e. without any scattering events) from heat source to sink (Sellan *et al.* [17]). When this occurs conductivites in shorter length cells are overestimated, reducing the gradient of the linear fit and thus underestimating the

extrapolated conductivity [[[I NEED TO HAVE SHOWN A FIGURE BY THIS POINT TO MAKE SENSE]]].

For a fixed cross-sectional area, conductivity increases with cell length ([23]). This can be observed on the inverse plot, where long cells exhibit increasing conductivity away from the linear region. The effect is due to relatively sparse phonon phase sampling in the cross-section compared to length, phonons that aren't resolved cannot contribute to phonon-phonon scattering effects. Unlike above, this divergence causes the gradient of a linear fit to increase and an overestimation to extrapolated conductivity. INCREASING CSA DOES NOT SUFFICIENTLY REDUCE THIS EFFECT - THIS STATEMENT GOES IN DISCUSSION?

A third effect of system size can cause an incorrect conductivity extrapolation, when the cross-sectional area is too small (Thomas *et al.* [24]? NANOTUBE DIAMETER RATHER THAN CSA). The effect of phonon-phonon scattering is underestimated in small area systems due to a restriction of the active phonon modes. Reduced scattering means heat transport is artificially more efficient than expected from the bulk material. The general effect of this on the inverse conductivity/length plot is a systematic shift of data towards higher conductivities (lower inverse conductivities?).

TWO CSA EFFECTS; LONG ASPECT RATIO IS UNDERSAMPLING, SMALL CSA IS TRUNCATION

(MOVE TO METHOD?) By comparing results with the Green-Kubo method, we will constrain the cell lengths in the linear extrapolation region to mitigate these effects.

(MOVE TO RESULTS?)We have investigated this effect by varying CSA for a range of cell lengths, extrapolated conductivity decreases and eventually converges with CSA. We will use the smallest area that produces the converged conductivity for computational efficiency.

C. Green-Kubo method (remove this subsection header later)

RETHINK FIGURES - WHICH DATA TO USE

TALK ABOUT GK FSE - WHAT AND WHY

The Green-Kubo method uses auto-correlation functions (ACFs) to quantify time-dependence of heat fluxes (shown in Figure **??**, and Equation 4), in a simulation cell of roughly cubic dimensions (WHY??) and spatially-consistent average temperature. Instan-

taneous heat fluxes can be used to determine how energy is dissipated within a system, where brief flux events mean heat is transferred quickly indicating high thermal conductivity (and vice versa). Auto-correlation is performed over the net heat flux series in each crystallographic direction, for a timescale up to a chosen correlation length.

$$ACF_i = \langle J_i(0) \cdot J_i(t) \rangle \,, \tag{4}$$

where i specifies direction, J is heat flux, and t is the correlation length. The integral of heat flux ACF is proportional to thermal conductivity via the Green-Kubo equation (see Figure **??** and Equation 5),

$$\kappa_i = \frac{V}{k_B T^2} \int_0^\infty \langle J_i(0) \cdot J_i(t) \rangle \, dt, \tag{5}$$

where V is the simulation cell volume, k_B is the Boltzmann constant, and T is the average temperature of the system. In this study we use Green-Kubo results as an independent check on the direct method, as they do not have the same finite size-effects. Obtaining a converged conductivity result simply depends on using a large enough cell volume / number of atoms.

The individual integrals obtained from the Green-Kubo show variation from the average combined integral on the order of the mean. Many simulations from different intital temperature conditions are required in order to ensure good sampling of conductivity, as well as ensuring the computation time for each is long enough for convergence. This makes Green-Kubo a computationally expensive method, especially for large systems.

The ACF should decay to zero as correlation time tends to infinity, however noise in the ACF prevents this. This will ultimately cause the integral to diverge/drift on long timescales. Howell [27] fits a series of exponential decays to their ACF, forcing the expected decay to zero and subsequent (constant) integral convergence. This is represents a significant improvement on the conductivity estimate at long correlation lengths, but is mostly similar with the un-fit integrals early in the correlation. (INTEGRAL DRIFT FIGURE, JUST THE ONE INTEGRAL FOR 100PS)

(STACKHOUSE 2010 REFERENCES Volz and Chen 2000; Sun and Murthy 2006)

III. METHODOLOGY

ENOUGH INFO FOR REPRODUCIBILITY !!!

WHAT I HAVE DONE / FOR REPRODUCIBILITY. SETUP STUFF, BUT CONDUCTIVITY / FINITE SIZE EFFECT RESULTS GO IN RESULTS SECTION

Using the classical molecular dynamics code LAMMPS(Plimpton [25]) (Large-scale Atomic/Molecular Massively Parallel Simulator), we calculate lattice thermal conductivities and constrain effects of finite simulation size. With the interatomic potential of Oganov *et al.* [26] we simulate bridgmanite ($MgSiO_3$ perovskite), the predominant phase in the lower mantle ($\sim$75%).

To assess the finite-size effects within bridgmanite, we use larger simulation cells than those employed in previous studies (BRIDG STUDIES OR FSE STUDIES?). The atom counts associated with these cells (the largest cell considered having over 100,000 atoms) means an ab initio study would be impractical, necessitating the use of interatomic potentials. We expect the potentials to represent the finite size effects well, even if computed conductivities may inaccurate compared to first-principles calculations.

WHY OGANOV?

WHAT CUTOFFS?

We present our approach for the direct and Green-Kubo methods, and show our calculations are converged with respect to simulation time (also temperature gradient and correlation length respectively - AWKWARD BRACKETS) [[[DO SIMULATION TIME CONVERGENCE FOR GK TOO]]]. The finite-size effect analysis for both methods can be found in Section. IV, along with a results comparison.

NPT-NVT-NVE PROCESS, BOTH METHODS

BAROSTAT-THERMOSTAT-SIMULATION

[[THIS PARAGRAPH IS DUMB, I DON'T THINK IT NEEDS TO BE IN PAPER]] We ensure all calculations are run for a sufficient length of time for the conductivity value to converge. When conductivity fails to converge it means either the simulations needs to be run for longer (unlikely with our nanosecond-scale classical calculations), or the system temperature has drifted. When NVE simulations are run for a long time there is noticable drift in the average system temperature (due to numerical approximations in the equation of motion), which in turn causes drift in the computed conductivity.

A. Direct method

The simulation supercell is split into sections along its length, each half a unit cell wide. Two of these sections, half the supercell length apart, are designated as the heat source and heat sink. We measure (HOW?) the temperature in all sections to obtain the temperature gradient. Heat flows in both directions from the hot section because of cell periodicity [NEED DIRECT METHOD DIAGRAM BY THIS PARA], meaning there are two temperature gradients to average. Where L is supercell length in unit cells and S (= 2L) gives the number of sections, we obtain S/2 + 1 temperature points to fit the gradient. Because the temperature gradient is non-linear around the heat source and sink, we ignore S/12 sections (rounded to nearest integer) from both ends of the temperature gradient. For a given simulation cell we fit S/3 + 1 points to obtain the temperature gradient. We use a minimum supercell length of 6 unit cells (12 sections, 5 data points), in order for sufficient fitting of the temperature gradient. [HOW NECESSARY IS THIS PARA, VERY JARGONY]

(MOVE TO RESULTS?) Changing the width of the heated sections has no effect on the conductivity result. Furthermore, changing the width (and thus number) of temperature bins has no effect on the sampled gradient, assuming resolution is large enough to capture the non-linear region around the heat source/sink.

An important factor for utilising the direct method is maintaining a sensible temperature gradient where Fourier's law remains valid, i.e. conductivity is constant along the length of the cell. Thermal conductivity is strongly temperature-dependent at upper lower-mantle conditions (1000 K), it is therefore undesirable to have substanially different conductivities as a of function of temperature across the cell. The opposite case is also true, the difference in temperature between hot and cold sections must be larger than the uncertainty in the average system temperature.

We typically observe fluctuations in temperature of around ±50 K during temperature equilibration, and look for temperature increases/decreases on the order of 10% the mean temperature. We control the magnitude of the gradient by altering the interval at which heat is exchanged. To produce the desired gradients we find shorter intervals are required as cell length decreases, cross-sectional area increases, and system equilibrium temperature decreases.

B. Green-Kubo method

The bridgmanite unit cell does not have cell dimensions resembling a cube (a:b:c = 1:1:1.4), so we use supercell structures of 3x3x2, 4x4x3, 5x5x4, 6x6x4 etc. to make an approximately cubic simulation cell. Temperature initialisation (NVT) of 1 ns is run to ensure convergence of system pressure and temperature. To obtain heat flux auto-correlation functions, a simulation for each initial temperature condition is run for X ns, with 9 successive repeats for a total of 10 jobs. This gives 10 ACFs from each initial condition. Simulation runs are split in this manner to be feasible computationally, and also to provide enough samples for ensemble averaging statistics (???).

3x3x2 - X = 10 ns, for 20 inital conditions - 2 μs total time

4x4x3 - X = 10 ns, for 30 inital conditions - 3 μs total time

5x5x4 - X = 5 ns, for 20 inital conditions - 1 μs, X = 1 ns, for 70 inital conditions - 0.7 μs, 1.7 μs total time

6x6x4 - X = 1 ns, for 80 inital conditions - 0.8 μs total time

THIS INFO IN A TABLE, OR JUST GIVE FOR THE RELEVANT VOLUME?

In this study we compute ACFs up to correlation lengths of 100 ps, with 1 fs timesteps. This length is longer than required but selected as a proof of concept to show convergence in the conductivity result, additionally to display the extent and behaviour of drift in the integrals for long correlation times. We show in Figure **??** that the magnitude of the ACF decays to much less than 1% of its initial value around a correlation time of 1 ps, inferring the start of convergence for the integral and thus conductivity. (ACF FIGURE FOR CORREL ¡ 10PS?, RUNNING AVERAGE SHOWS CONVERGENCE)

ACFs produced by each simulation are integrated seperately, after which the integrals are averaged into a single series with uncertainty (standard deviation of the mean, **??**). This process is performed for heat fluxes in each crystallographic direction, allowing analysis of anisotropy and finite system size effects. We obtain a conductivity value from the combined integral by averaging a window between correlation times of 2-10 ps (for 136 GPa, 4000 K [THIS WILL NEED TO BE CHANGED]). Windows are chosen to capture a flat, converged region of the integral, or the section just after the 'bottleneck' if convergence is not obvious (**??**, but show window, and example of bottleneck?). We find correlation time of 2-10 ps to be long enough for good sampling of the integral, and short enough to ignore the aforementioned

drift-effects. (INTEGRAL FIGURE WITH UNCERTAINTY FOR ¡10PS?, POINT TO CONVERGENCE, SHOW SMALL ZOOM OUT OF SAME GRAPH UP TO 100PS. SOME WAY TO COMBINE WITH ABOVE FIGURE)

AAARRGH!!! - CONVERGENCE OF KAPPA WITH SIMULATION TIME - AAARRGH!!!

DONT NEED ALL THESE GRAPHS

IV. RESULTS

LOTS OF QUANTIFYING

A. Green-Kubo method

A supercell volume of 3x3x2 (((REFER TO GRAPH, WILL NEED 1000K TOO))) fails to reproduce conductivities on the same order as the larger cells for all directions. We identify 4x4x3 and larger cells as being converged with respect to cell volume (((PROBLEMATIC STATEMENT, NOT CONVINCING, BY WHAT METRIC?))). This a useful result in terms of computation efficiency, as 6x6x4 supercells are 3 times as large (VOLUMOUS? REFERENCE ATOM COUNT?) as 4x4x3. Whereas here our error bars represent statistics on the integrals, the errors we take on results from 4x4x3 cells going forward will be related to the variation with the larger cells ((THIS IS OBVIOUS NONSENSE, HAVE TO CHANGE)).

B. Direct method

MFP DEPENDENT FSE, PROVE DIFFERENCE.

When determining finite-size effects, it is important to consider the scenario with largest phonon mean-free paths. Phonon MFPs are largest at low temperatures (beyond the Debye temperature) and high pressures. In light of this we consider pressure of 136 GPa and temperatures of 1000 K and 4000 K. 136 GPa / 4000 K represents the expected conditions of the core-mantle boundary, whereas 136 GPa / 1000 K is unphysical in the context of the Earth but maximises MFP. UPDATE - GK RUINS EVERYTHING

By computing conductivities across a range of cell lengths we show that direct method simulations with small cross-sectional areas fail to produce converged results with respect to larger CSAs. Without considering any extrapolation, it is clear that small CSA cells overestimate conductivity (Figures **??** & **??**) at conditions of both 1000 K and 4000 K. On both figures the results for cells with CSA 2x2 and larger plot close to on top of each other. Producing the same results as 8x8 cells, we conclude that cells with CSA of 2x2 are suitable for direct method simulations of bridgmanite.

Now considering CSAs of 2x2, we examine the divergence of conductivity result with cell length from an expected linear trend (Figure **??**). As mentioned in Section II B, cells that are too long or short cause a conductivity result to be overestimated. At 4000 K we find that cells up to 24 unit cells length (<0.06 in inverse length) produce a reasonably linear trend. At this condition, there is no reasonable overestimation due to short cells and ballistic phonon transport. However at 1000 K where the MFP is longer, a cell of length 6 unit cells (inverse length 0.167) produces conductivity larger than expected. The same long-cell divergence is found >24 unit cells length, the onset of insufficient phonon sampling. For all direct method simulations of bridgmanite at lower mantle conditions, we recommend employing cell lengths of 8 - <24 unit cells. Due to the increasing computational cost associated with cell length (especially for ab initio methods), we recommend the longest cells be 16 unit cells. FINITE SIZE EFFECTS INCREASE WITH MFP/KAPPA

Now we consider CSA of 2x2 and supercell lengths of 8, 10, 12, and 16 unit cells for comparison with the results from Green-Kubo. After performing a weight least squares regression (extrapolation) on the direct method results, we obtain a conductivity with uncertainty. Figure **??** shows the extrapolation and Green-Kubo result (at x = 0). They agree within error, meaning we have chosen a suitable set of criteria for working with direct method results. DO I NEED TO PROVE THAT OTHER LENGTHS/EXTRAPOLATIONS DON'T MATCH GK?

SCALING LAW / THEORETICAL MODEL

PROBABLY SHOULD MENTION THE VALUE OF THE RESULT?

PREVIOUS WORK :(

V. SUMMARY AND CONCLUSION

For bridgmanite (at conditions representing the lower mantle), we show that use of the direct method for calculation of thermal conductivity will lead to an overestimate if the simulation cell is too long (>16 unit cells). Small cross-sectional areas (<2x2 unit cells) also overestimate the thermal conductivity. This informs future work using Density Functional Theory, and will allow a model of lower mantle conductivity considering composition to be established.

(ASSUMING THE RESULTS ARE CORRECT AND AGREE WITH GK) We see the non-linear region as described by Sellan *et al.* [17] for the cell length of 6 unit cells at 1000 K, which has individually higher conductivity than expected from the linear fit through data points corresponding to lengths of 8-16 unit cells. When included in the extrapolation, this reduces the gradient of the fit, raising the intercept and thus causing conductivity to be underestimated. At temperature of 4000 K, the 6 length cell is inline with the fit through other cells with length less than 16 unit cells. As the ratio of cell length to phonon MFP increases with temperature, we believe the onset of divergence as described by Sellan et al. moves to the right (??? - MENTION ACTUAL EFFECT - QUANTIFY RATHER THAN REFERENCING GRAPH). A shorter MFP needs shorter cell lengths to display divergent conductivity, of which we have not sampled (at high temperature). DOING THE DIRECT METHOD WITH CELLS OF LENGTH LESS THAN 6 UNIT CELLS AT ANY TEMPERATURE IS A BAD IDEA BECAUSE ...

We find conductivity is definitely dependent on CSA, but we were not able to increase CSA enough to eliminate aspect ratio-dependent divergence as reported by Hu *et al.* [23]. This does support our conclusion ignoring long cell lengths however, in order to keep the aspect ratio within a reasonable limit and ensure a linear fit is extrapolated. (EVEN THOUGH 48x8x8 HAS A SMALLER RATIO than 8x2x2?)

(WAFFLE ALERT) Ignoring the specifics of this study, we stress the importance of performing finite-size analysis when performing direct method calculations. Direct method cells spanning a range of lengths must be considered to find the linear regime for extrapolation. Cross-sectional area must be increased until the conductivity result converges. The same can be said about the Green–Kubo method, where the result converges with increasing volume. These effects vary with phonon mean-free path, sensitive to pressure, temperature,

and compositional variations such as impurities. Completing finite-size effect analysis at conditions with the largest phonon mean-free path / thermal conductivity ensure all other conditions represent converged results. We believe classical molecular dynamics with interatomic potentials to be an excellent way of quantifying these effects quickly, performing ab initio methods (SHOULD I TAKE THIS SENTENCE OUT, NO PROOF OF THIS CLAIM).

FUTURE WORK?

ACKNOWLEDGMENTS

Thank you NERC

"We also acknowledge the use of high performance computing provided by Advanced Research Computing at the University of Leeds."

ANDREW HAS SOMETHING TO ADD (AMW IRF from NERC w/ grant code)

STEPHEN HAS SOMETHING TO ADD (LLSVP Grant from NERC / MSRC / ????)

[1] N. Tosi, D. A. Yuen, N. de Koker, and R. M. Wentzcovitch, Physics of the Earth and Planetary Interiors **217**, 48 (2013).

[2] G. J. Snyder and E. S. Toberer, Nature materials **7**, 105 (2008), arXiv:1512.00567.

[3] T. Lay, J. Hernlund, and B. A. Buffett, Nature Geoscience **1**, 25 (2008).

[4] J. M. Brown and R. G. McQueen, Journal of Geophysical Research **91**, 7485 (1986).

[5] M. Osako and E. Ito, Geophysical Research Letters **18**, 239 (1991).

[6] A. M. Hofmeister, Science **283**, 1699 (1999).

[7] A. F. Goncharov, P. Beck, V. V. Struzhkin, B. D. Haugen, and S. D. Jacobsen, Physics of the Earth and Planetary Interiors **174**, 24 (2009).

[8] G. M. Manthilake, N. de Koker, D. J. Frost, and C. A. McCammon, Proceedings of the National Academy of Sciences of the United States of America **108**, 1 (2011).

[9] K. Ohta, T. Yagi, N. Taketoshi, K. Hirose, T. Komabayashi, T. Baba, Y. Ohishi, and J. Hernlund, Earth and Planetary Science Letters **349-350**, 109 (2012).

[10] S. Stackhouse and L. Stixrude, Reviews in Mineralogy and Geochemistry **71**, 253 (2010).

[11] M. S. Green, The Journal of Chemical Physics **22**, 398 (1954).

[12] R. Kubo, Journa; of the Physical Society of Japan **12** (1957), 10.1143/JPSJ.12.570.

[13] R. Kubo, Reports on Progress in Physics **29**, 255 (1966).

[14] P. K. Schelling, S. R. Phillpot, and P. Keblinski, Physical Review B **65**, 144306 (2002).

[15] F. Muller-Plathe, The Journal of Chemical Physics **106**, 6082 (1997).

[16] C. Nieto-Draghi and J. B. Avalos, Molecular Physics **101**, 2303 (2013).

[17] D. P. Sellan, E. S. Landry, J. E. Turney, A. J. H. McGaughey, and C. H. Amon, Physical Review B **81**, 1 (2010).

[18] M. W. Ammann, A. M. Walker, S. Stackhouse, J. Wookey, A. M. Forte, J. P. Brodholt, and D. P. Dobson, Earth and Planetary Science Letters **390**, 175 (2014).

[19] S. Stackhouse, L. Stixrude, and B. B. Karki, Earth And Planetary Science Letters **427**, 11 (2015).

[20] V. Haigis, *Trace elements in silicate melts and the thermal conductivity of the earth's deep mantle: insights from atomistic modeling of geomaterials*, Ph.D. thesis, Freien Universität Berlin (2013).

[21] X. Tang, M. C. Ntam, J. Dong, E. S. G. Rainey, and A. Kavner, Geophysical Research Letters **41**, 2746 (2014).

[22] H. Dekura, T. Tsuchiya, and J. Tsuchiya, Physical Review Letters **110**, 1 (2013).

[23] L. Hu, W. J. Evans, and P. Keblinski, Journal of Applied Physics **110**, 113511 (2011).

[24] J. A. Thomas, R. M. Iutzi, and A. J. H. McGaughey, Physical Review B - Condensed Matter and Materials Physics **81**, 1 (2010).

[25] S. Plimpton, Journal of Computational Physics **117**, 1 (1995).

[26] A. R. Oganov, J. P. Brodholt, and D. G. Price, Physics of the Earth and Planetary Interiors **122**, 277 (2000).

[27] P. C. Howell, The Journal of chemical physics **137**, 224111 (2012).

FIGURE CAPTIONS

FIG. 1. Normalised ACF. Correlation is taken over a longer length than shown on this plot (10 ps, see Figure 8 below), however the function decays to less than 1% of its initial value at 2 ps. It continues to oscillate about zero, with a positive average value.

FIG. 2. Integrated ACF, multiplied by constants to get thermal conductivity. Large variation in the first 1 ps corresponds to the correlation time where the ACF is unconverged (still decaying / large oscillations). Thermal conductivity is averaged from correlation time of 5 ps - 10 ps (region in red box).

FIG. 3. normalised acf in percent against 2ps correl. 1 on y-axis = 1%

FIG. 4. kappa against 100ps correl

FIG. 5. kappa w/ uncertainty against 100ps correl. green series is all runs from each initial condition combined

FIG. 6. kappa w/ uncertainty against 10ps correl. shorter time scale than previous figure. flat region from 4-10ps. DON'T NEED ALL THESE GK FIGURES

FIG. 7. kappa vs. volume, all directions. dashed lines show values at 4x4x3, the chosen volume, for comparison. change x-axis to atom count, or number of constituent cell?

FIG. 8. inverse conductivity against inverse length at 4000K. each series is a different CSA

FIG. 9. inverse conductivity against inverse length at 1000K. each series is a different CSA. COULD TRY AND COMBINE THESE FIGURES, SIMILAR Y-AXIS, MIGHT BE MESSY

FIG. 10. off-colour data points are not fit. Although the 1000 K data points look closer to the linear trend, they are further in magnitude due to the nature of the inverse y-axis.

FIG. 11. MAKE THIS INTO A LATEX TABLE OBVIOUSLY

FIG. 12. The results of Figure 9 for cross-section of 2x2 and lengths 16 unit cells. Diagrams of cell geometry are shown, with dimensions in unit cells and the number of atoms. Green-Kubo result is plotted on the y-axis for comparison with extrapolated direct method conductivity. WEIGHTED FIT DOESN'T LOOK LINEAR, INCREASE Y-AXIS RANGE?

FIGURES

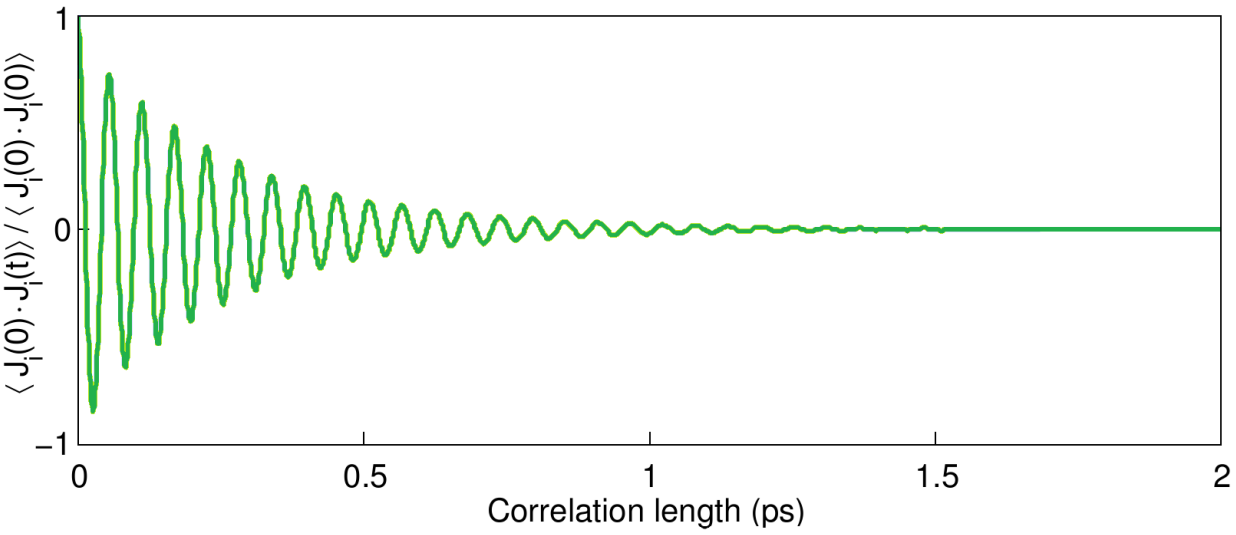

FIG. 1. Normalised ACF. Correlation is taken over a longer length than shown on this plot (10 ps, see Figure 8 below), however the function decays to less than 1% of its initial value at 2 ps. It continues to oscillate about zero, with a positive average value.

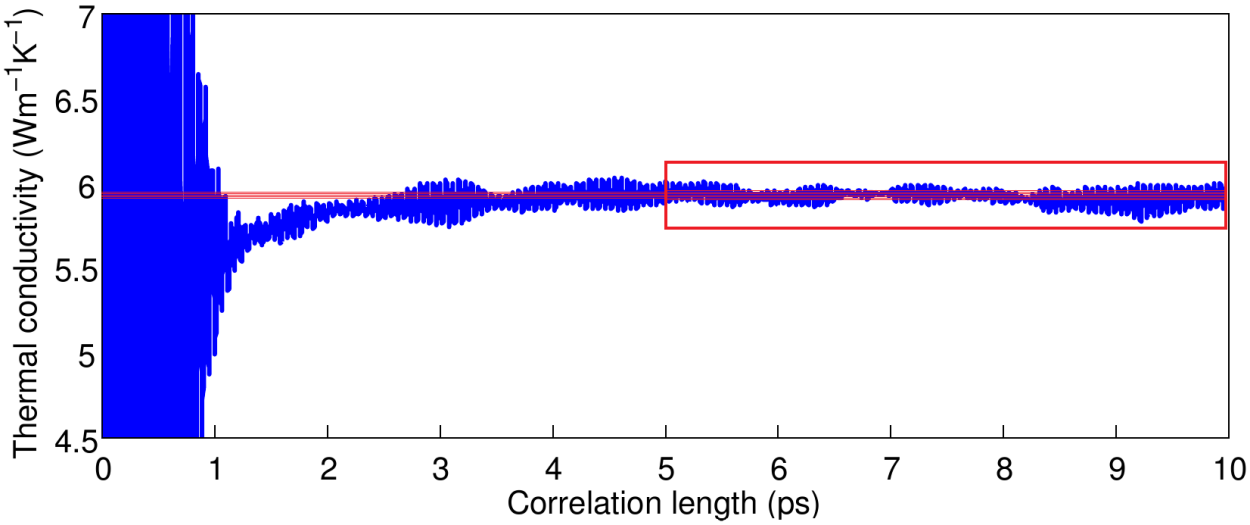

FIG. 2. Integrated ACF, multiplied by constants to get thermal conductivity. Large variation in the first 1 ps corresponds to the correlation time where the ACF is unconverged (still decaying / large oscillations). Thermal conductivity is averaged from correlation time of 5 ps - 10 ps (region in red box).

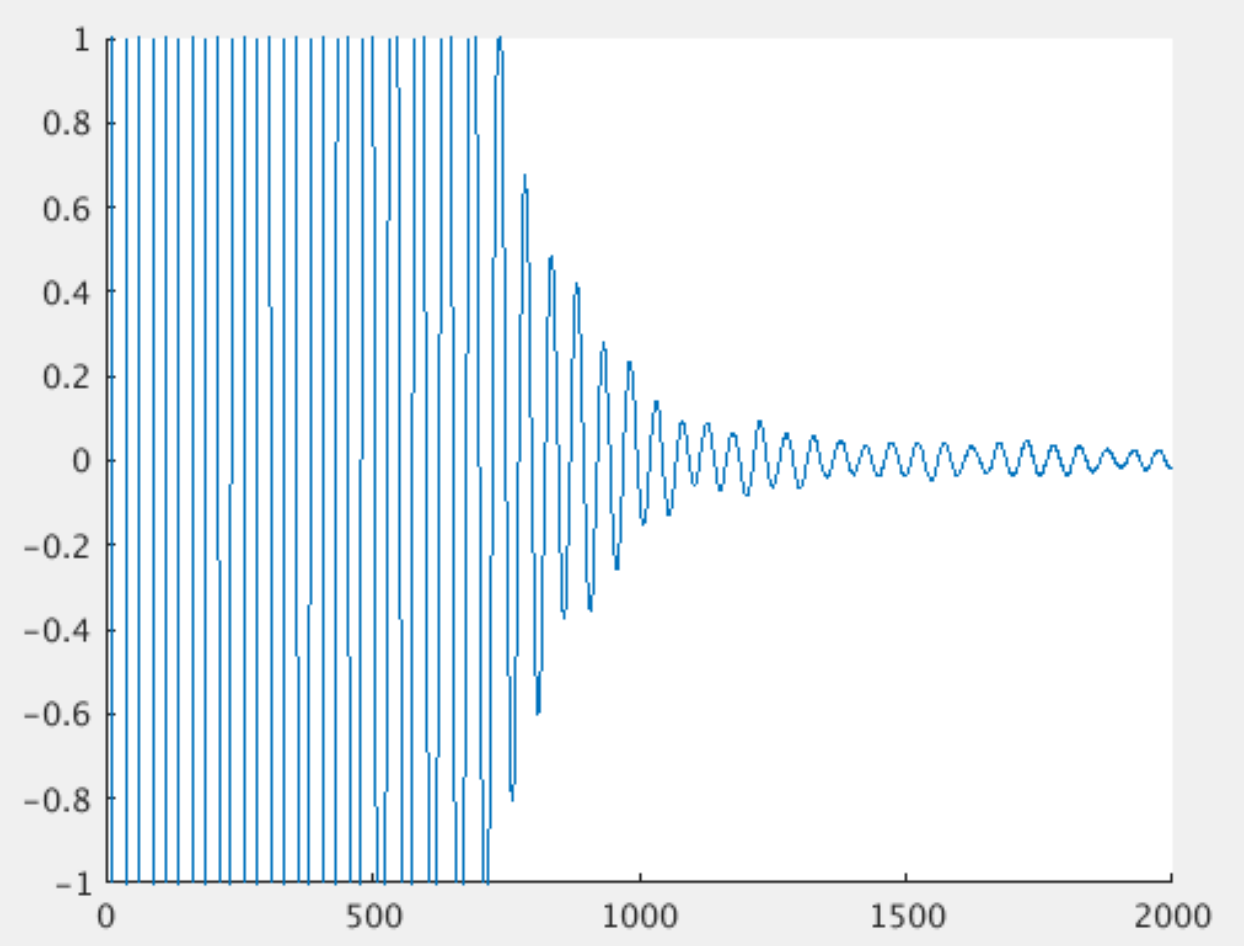

FIG. 3. normalised acf in percent against 2ps correl. 1 on y-axis = 1%

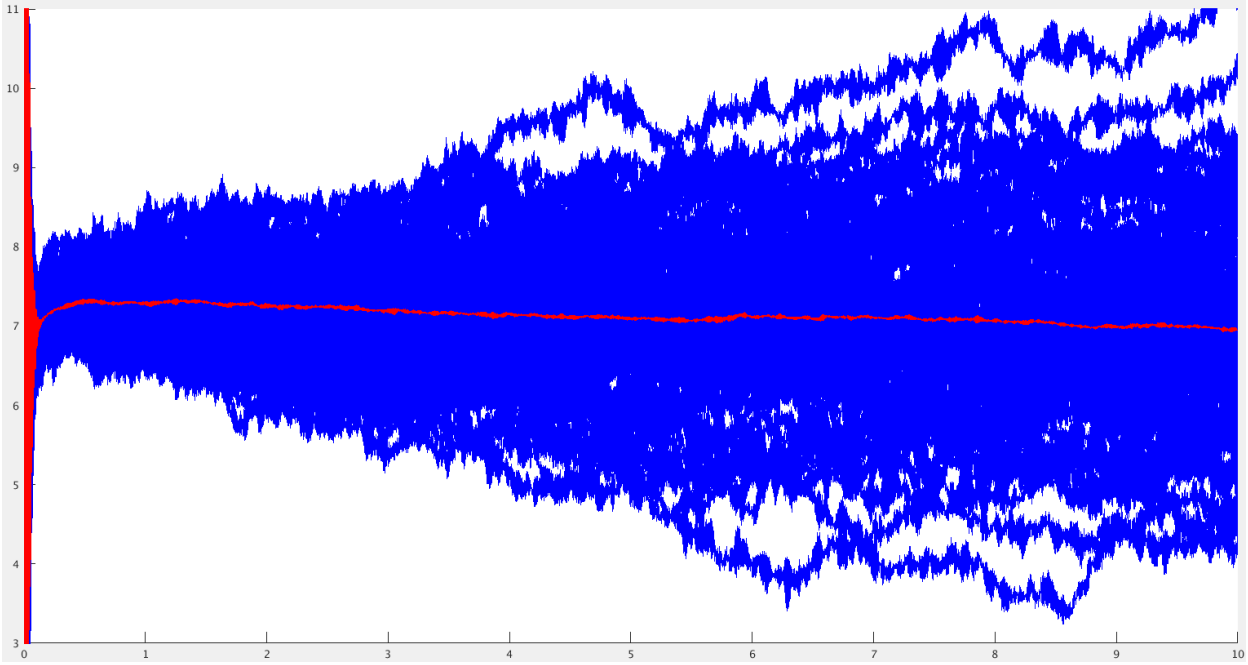

FIG. 4. kappa against 100ps correl

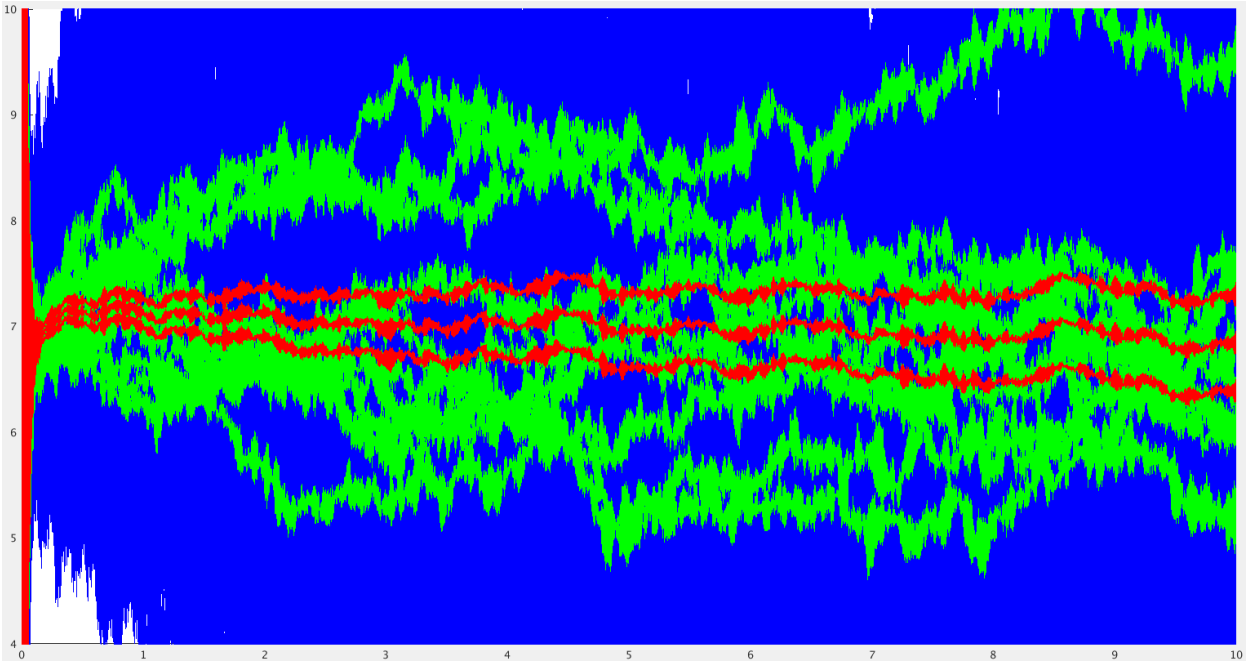

FIG. 5. kappa w/ uncertainty against 100ps correl. green series is all runs from each initial condition combined

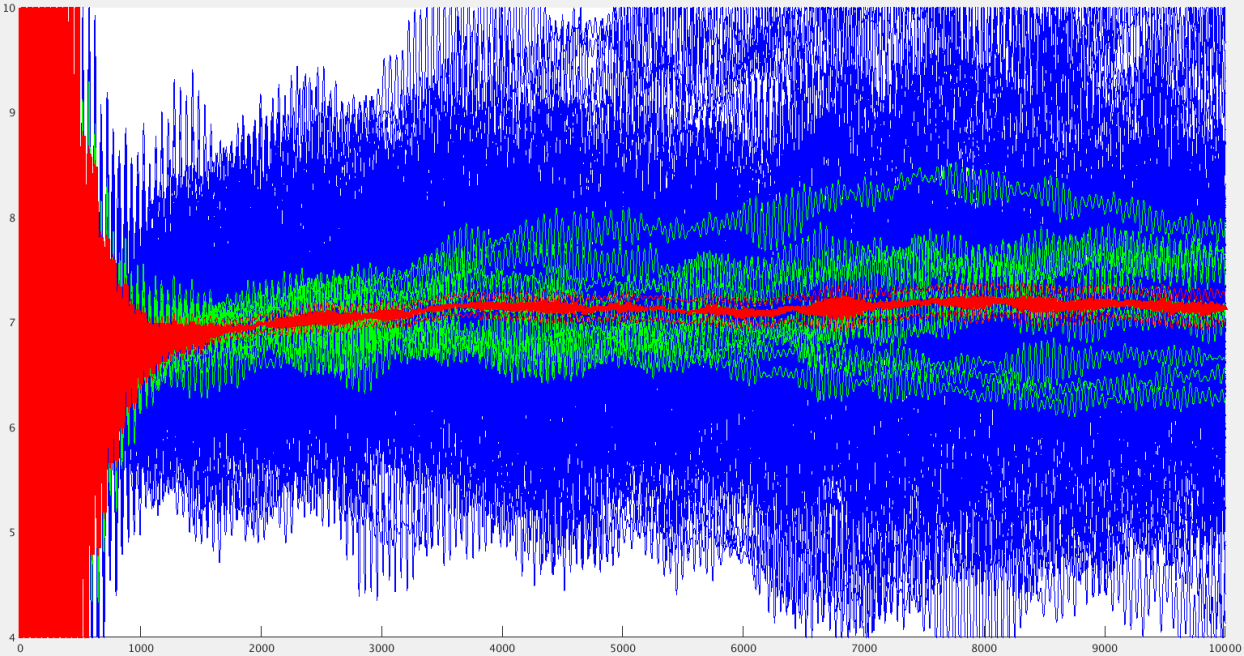

FIG. 6. kappa w/ uncertainty against 10ps correl. shorter time scale than previous figure. flat region from 4-10ps. DON'T NEED ALL THESE GK FIGURES

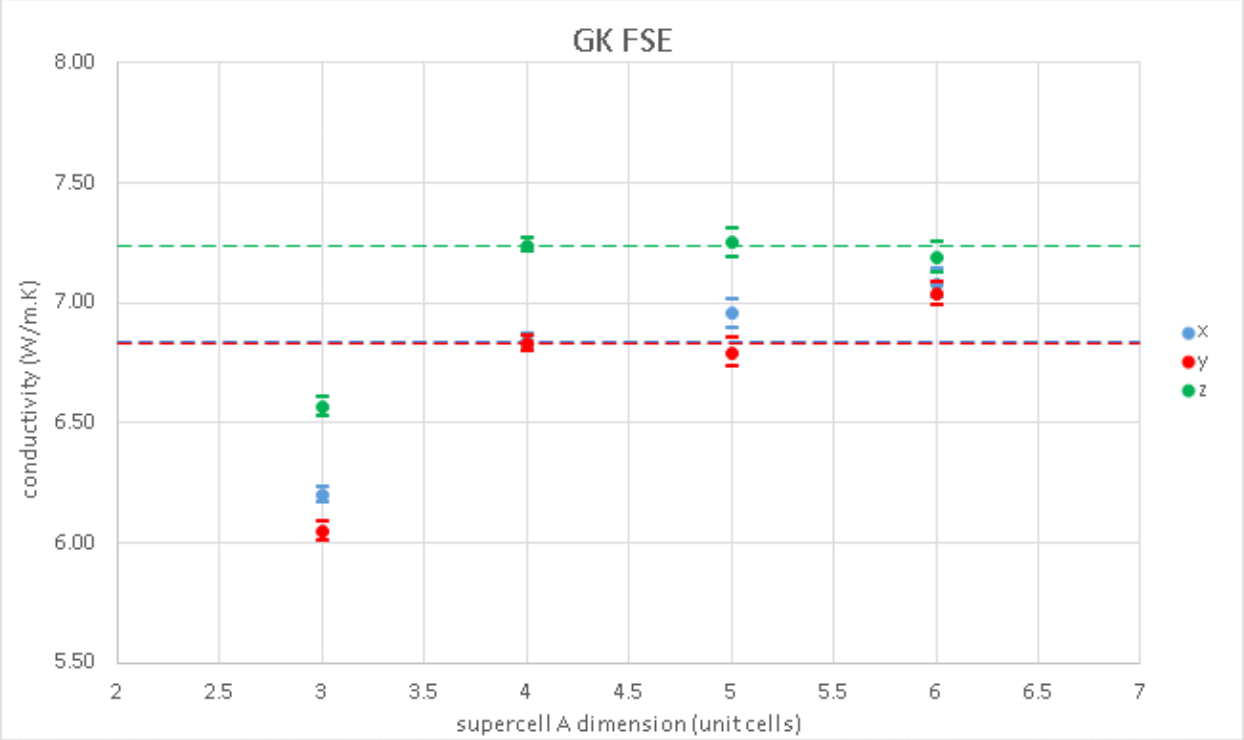

FIG. 7. kappa vs. volume, all directions. dashed lines show values at 4x4x3, the chosen volume, for comparison. change x-axis to atom count, or number of constituent cell?

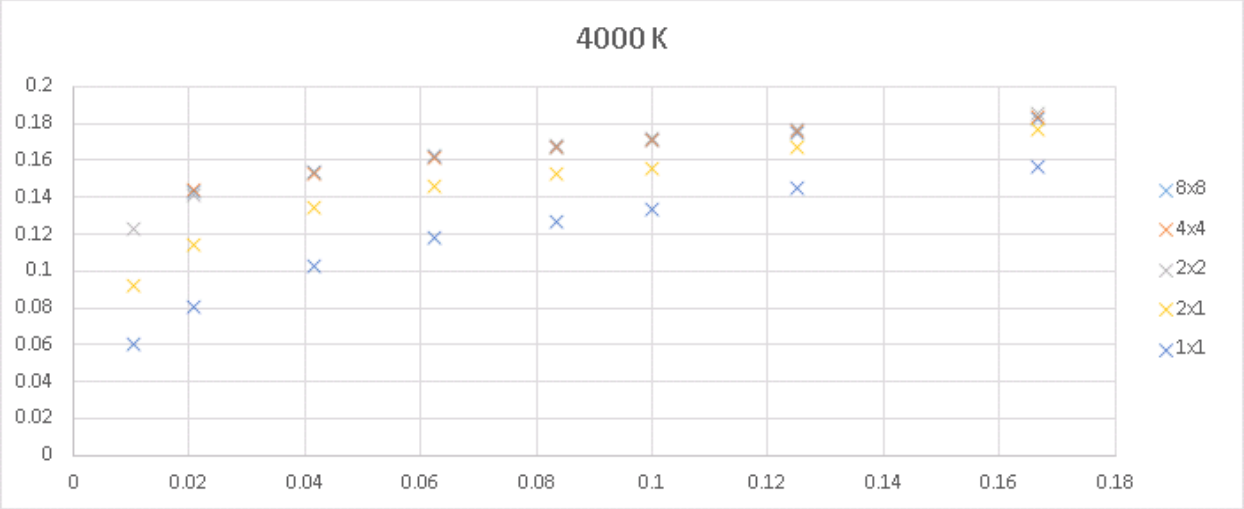

FIG. 8. inverse conductivity against inverse length at 4000K. each series is a different CSA

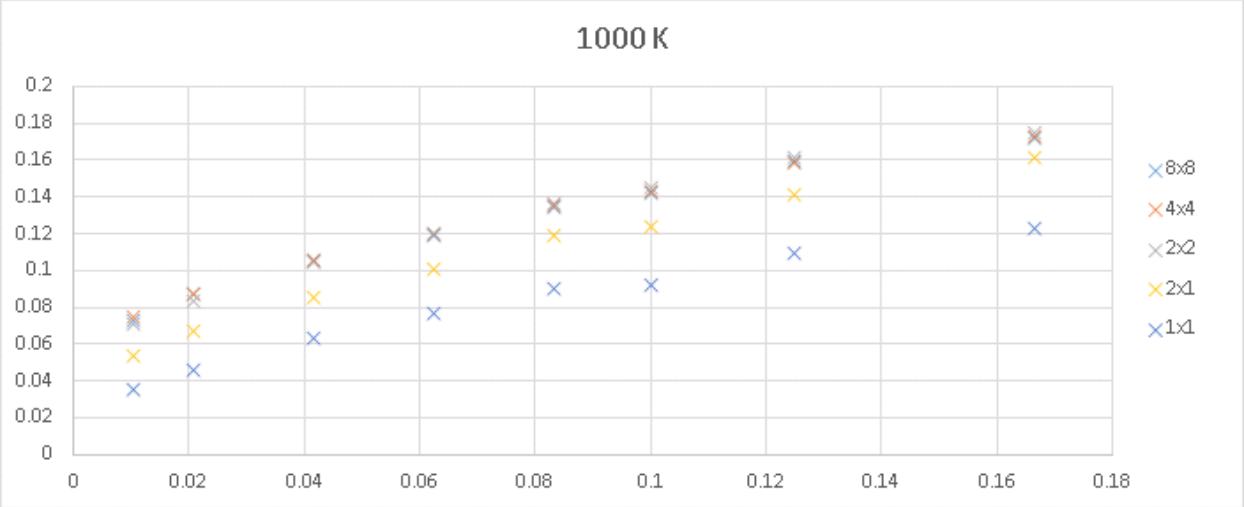

FIG. 9. inverse conductivity against inverse length at 1000K. each series is a different CSA. COULD TRY AND COMBINE THESE FIGURES, SIMILAR Y-AXIS, MIGHT BE MESSY

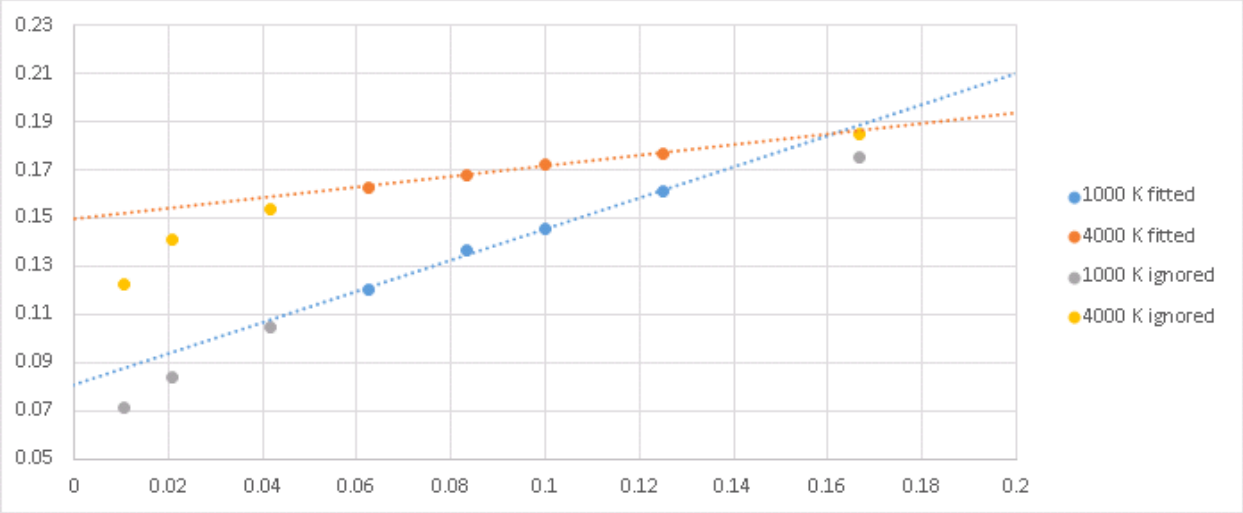

FIG. 10. off-colour data points are not fit. Although the 1000 K data points look closer to the linear trend, they are further in magnitude due to the nature of the inverse y-axis.

		ignored	included	-	-	included	ignored	-	-
cell length	real	6	8	10	12	16	24	48	96
(unit cells)	inverse	0.17	0.13	0.10	0.08	0.06	0.04	0.02	0.01
divergence from fit	4000 K	0.12	0.05	-0.03	-0.04	-0.06	0.08	0.43	1.37
(conductivity)	1000 K	0.46	0.04	0.00	-0.12	0.00	0.10	1.10	2.30

FIG. 11. MAKE THIS INTO A LATEX TABLE OBVIOUSLY

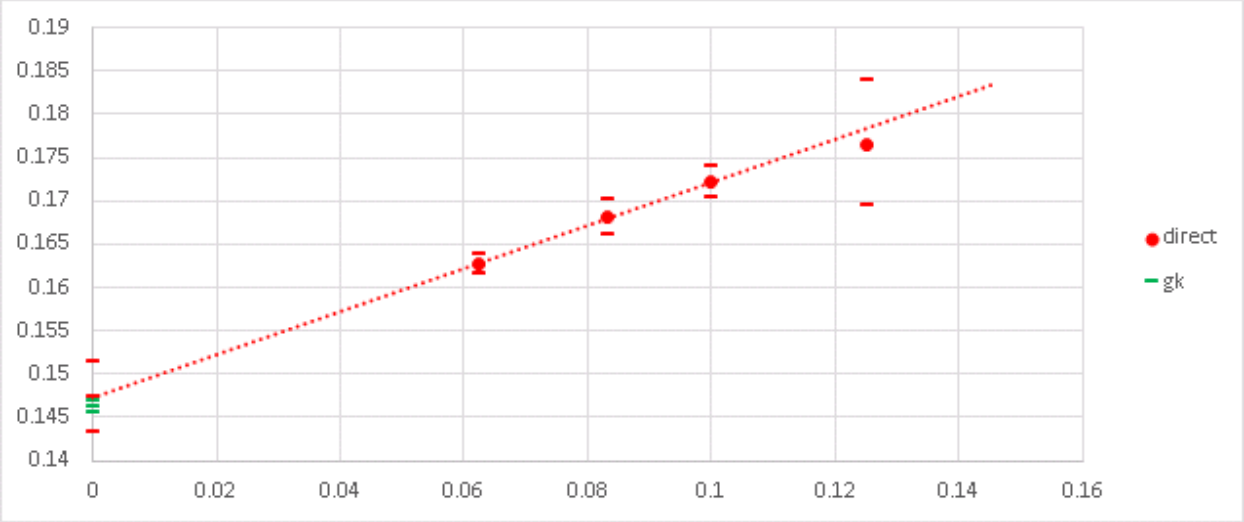

FIG. 12. The results of Figure 9 for cross-section of 2x2 and lengths 16 unit cells. Diagrams of cell geometry are shown, with dimensions in unit cells and the number of atoms. Green-Kubo result is plotted on the y-axis for comparison with extrapolated direct method conductivity. WEIGHTED FIT DOESN'T LOOK LINEAR, INCREASE Y-AXIS RANGE?